Brown Adipose Tissue with Low Fat Content in Newborns with Hypothermia

Houchun Harry Hu[1], Tai-Wei Wu[2], Larry Yin[3], Mimi S. Kim[3], Jonathan M. Chia[4], Thomas G. Perkins[4], and Vicente Gilsanz[1]

[1]Radiology, Children's Hospital Los Angeles, Los Angeles, California, United States, [2]Neonatology, Children's Hospital Los Angeles, Los Angeles, California, United States, [3]Pediatrics, Children's Hospital Los Angeles, Los Angeles, California, United States, [4]Philips Healthcare, Cleveland, Ohio, United States

▪ **Target Audience:** Investigators engaged in water-fat MRI and brown adipose tissue research.

▪ **Purpose: We report findings of brown adipose tissue (BAT) with low fat content in hypoxic-ischemic encephalopathy (HIE) neonates after hypothermia therapy (HT).** HIE is a condition in newborns in which the blood and oxygen supply to the brain are interrupted. Consequently, the risk of neurological deficit and injury, respiratory failure, depression of muscle tone and reflexes, unconsciousness, and seizure increases. HT is a treatment for newborns with moderate/severe HIE. It involves ***actively cooling*** the body core temperature to 33°C for ~48h. Its purpose is to attenuate secondary energy failure and to reduce the ensuing incidence of neurological disability and death [1].

BAT is implicated in non-shivering thermogenesis and the regulation of core body temperature. The tissue consumes intracellular fat to generate heat. Studies have shown an increase in BAT thermogenic activity and a reduction in intracellular fat content in cold-exposed animals [2-4]. We hypothesize herein that HIE neonates exhibit BAT depots with low fat stores as a response to HT cold-exposure.

▪ **Methods:** The use of water-fat MRI and the fat-signal fraction **(FF)** metric to characterize BAT has been described [5,6]. BAT has a lower FF than white adipose tissue and elevated BAT metabolic activity leads to the expenditure and subsequent depletion of intracellular fat, and consequently a lower tissue FF [7]. ▪ ***Cohort*** - Ten full-term HIE newborns undergoing HT were studied (Table 1, Subject #1-10). In each subject, HT duration was set for 48h using a water-based active temperature regulation system (Blanketrol III, Cincinnati Sub-Zero Products, Inc.). HT was initiated upon hospital admittance, typically within a few hours to one day after birth. During the last hour of HT, each patient was transported to MRI for a neural exam. The Blanketrol system was operational during transport and subsequently during MRI. At the time of MRI, all ten neonates were between two to three days of life and were under stable conditions. We also recruited five non-HIE neonates in an effort to provide some level of comparison (Table 1, Subject #11-15). ▪ ***Water-Fat MRI*** - All exams were performed on a 3T system (Achieva TX, R3.2, Philips Healthcare). For the HIE subjects, a neonatologist determined the need for sedation. All non-HIE subjects were imaged during sleep without sedation. A multi-echo water-fat strategy (mDIXON) was utilized. Data were acquired with an 8-channel pediatric head-spine array. Imaging parameters for the 3D SPGR sequence included: TR=8-9ms, 1st TE=1.2-1.4ms, ΔTE=1.1-1.2ms, six echoes, bipolar readout, 1mm in-plane resolution, FOV= 20-24cm, 75-125 coronal 2mm overlapping slices, flip angle=3°, BW=1.3kHz/pixel, and 2x R/L SENSE, scan time=80-120s. For data reconstruction, we used a 6-peak fat spectral model pre-calibrated from ex vivo murine BAT [8]. The default system setting is based on a 7-peak model [9]. ▪ ***FF Analysis*** - We focused on quantifying FF in the supraclavicular BAT depots using previously described manual segmentation procedures [10]. A pediatric radiologist delineated the outlines of the entire supraclavicular BAT area on every mDIXON slice where the depots were visible, along with adjacent areas that needed to be excluded during segmentation, including major arteries and veins, bone and bone marrow, and muscles. An operator then used sliceOmatic software (Tomovision, Inc.) to manually segment both the left and right BAT depots. Region-of-interest FF distributions were then computed.

▪ **Results:** The right-most two columns of Table 1 summarize supraclavicular BAT depot volume and FF measurements, respectively. No statistical difference in the depot volume (p=0.12) was found between the two groups. FIG.1 illustrates a scatterplot of BAT FF, showing evident group differences. FIG.2 illustrates FF maps on a rainbow color scale in a non-HIE neonate. Note clear visualization of the bilateral supraclavicular BAT depots in green (arrows). For comparison, FIG.3 shows FF maps from HIE Subjects #1 and #9. Relative to the non-HIE case in FIG.2, note the heterogeneous appearance of the depots in Subject #1 and the near fat-depleted appearance (low FF) in Subject #9. FIG.4 shows axial reformatted FF maps of Subjects #3, #4, and #2, presented in this order to show progressively increasing FF values within the supraclavicular BAT depot. The contours circumscribe the BAT depots and are drawn for illustration purposes only. Note the very low FF appearance in Subjects #3 and #4.

▪ **Discussion/Conclusion:** The concept of fat-depleted BAT is not new. It has been previously reported in malnourished children [11], in post-mortem bodies whose cause of death included traumatic events such as burning, drowning, bleeding, and drug poisoning [12], and in infants who were undersized and pre-mature at birth, as well as those who suffered from respiratory distress, cold syndrome, congenital heart disease, and gastrointestinal complications [13,14]. It is known that at birth, newborns anticipate a cold-exposure to ambient temperature upon removal from the intrauterine environment. Since newborns are incapable of shivering due to the lack of neural and musculoskeletal development, BAT-mediated non-shivering thermogenesis represents the primary pathway for heat generation. We posit that HIE newborns undergoing HT are subjected to *additional* cold-stress that consequently leads to the depletion of intracellular fat reservoirs within their brown adipocytes. Conversely, it can also be argued that the presence of depleted BAT in utero may have led to the onset of HIE. Indeed, several reports have alluded to a link between BAT dysfunction and sudden infant death syndrome [15,16]. In conclusion, we believe that low FF measurements reflect a physiologically realistic scenario of fat-expended BAT, implying the tissue's recent involvement in high levels of oxidative metabolism and thermogenesis.

#	Gender	Age at MRI (days)	Rectal Temperature During MRI (°C)	Supraclavicular BAT	
				Volume of Depot (ml)	FF mean ± SD (%)
HIE Cohort					
1	M	2	33.0	8.3	29.9 ± 6.6
2	F	2	32.9	5.9	25.9 ± 7.5
3	F	2	32.6	2.2	12.9 ± 3.3
4	F	2	33.4	2.1	18.2 ± 3.7
5	F	2	32.4	6.8	10.3 ± 5.8
6	F	2	33.2	4.0	11.9 ± 3.7
7	F	3	33.8	2.5	14.0 ± 4.9
8	M	3	33.0	2.2	24.7 ± 6.3
9	M	3	33.2	10.7	11.6 ± 3.4
10	F	3	33.5	7.3	13.6 ± 6.3
non-HIE Cohort					
11	M	2	na	15.0	42.2 ± 8.0
12	M	3	na	7.5	23.7 ± 6.0
13	F	1	na	5.1	31.9 ± 10.3
14	M	6	na	5.0	24.4 ± 8.8
15	F	6	na	8.7	26.6 ± 6.9

Table 1: Summary of HIE (#1-10) and non-HIE (#11-15) quantitative measurements.

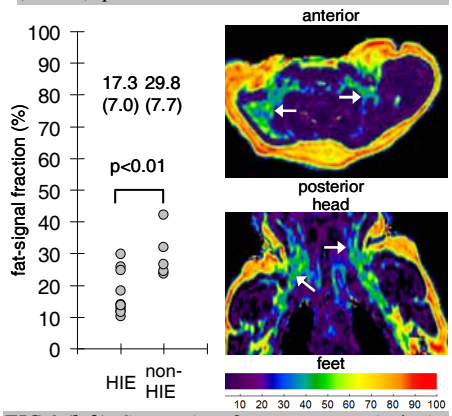

FIG.1 (left): Scatterplot of average supraclavicular BAT fat-signal fraction. Group standard deviations are given in parenthesis. Two-tailed *t*-test yields statistical significance. ***FIG.2 (right):*** Exemplary axial *(top)* and coronal *(bottom)* fat-signal fraction maps in a non-HIE neonate (Subject #11). Arrows denote bilateral supraclavicular BAT depots.

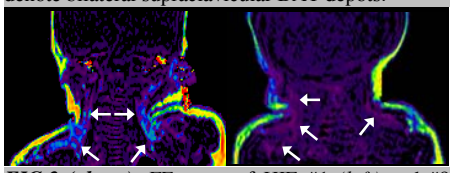

FIG.3 (above): FF maps of HIE #1 *(left)* and #9 *(right)*. ***FIG.4 (below):*** FF maps of HIE #3 *(left)*, #4 *(middle)*, and #2 *(right)*. Same scale as FIG.2.

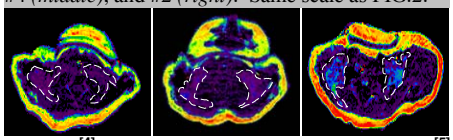

[1] Azzopardi. *NEJM* 2009;361:1349. [2] Cameron. *J Cell Biol* 1964;23:89. [3] Smith. *Am J Physiol* 1964;206:143. [4] Dawkins. *J Physiol* 1964;172:216. [5] Holstila. *Metabolism* 2013;62:1189. [6] Chen. *J Nucl Med* 2013;54:1584. [7] Smith. *JMRI* 2013; PMID: 23580443. [8] Hamilton. *JMRI* 2011;34:468. [9] Ren. *J Lip Res* 2008;49:2055. [10] Hu. *JMRI* 2013; PMID: 23440739. [11] Brook. *J Physiol* 1973;223:75. [12] Tanuma. *Arch Histol Jpn* 1976;39:117. [13] Aherne. *J Pathol Bacteriol* 1966;91:223. [14] Heaton. *J Pathol.* 1973;110:105. [15] Reid. *Med Hypotheses* 1994;42:245. [16] Lean. *J Clin Pathol* 1989;42:1153.